

Radiation and intensity-modulated radiotherapy for metastatic spine tumors

Marie D. Klish, MD*, Gordon A. Watson, MD, PhD,
Dennis C. Shrieve, MD, PhD

*Department of Radiation Oncology, University of Utah Hospital, 50 North Medical Drive,
Room B050, Salt Lake City, UT 84132–1801, USA*

Intensity-modulated radiotherapy background and historical perspective

Historically, radiotherapy treatment planning and delivery was based on two-dimensional imaging. The field borders for such traditional plans were typically based on bony anatomic landmarks as seen on plain films. Relatively recent advances in computer hardware and software have enabled the implementation of three-dimensional conformal radiation treatment (3D-CRT), which uses planning computed tomography (CT) scans or magnetic resonance imaging. This enables more accurate definition of target and avoidance volumes in three dimensions. This is clearly an advantage when treating spinal tumors, because the target volume can be more precisely defined in relation to the vertebrae, dura, and spinal cord. In 3D-CRT treatments, a set of fixed radiation beams is delivered, with each shaped to the projection of the target volume using a “beam’s eye view.”

Stereotactic radiosurgery (SRS) is a specific type of 3D-CRT that uses highly conformal beams to deliver an ablative dose of radiation to a target in one fraction [1]. Normal tissue exposure is kept at a safe level by using multiple cross-fired beams all focused on the target. Any given area of normal tissue is traversed by only one beam and thus receives only a small fraction of the target dose. Radiosurgery has been successful in

treating a wide range of intracranial and, more recently, extracranial lesions. In conventional 3D-CRT and SRS, each radiation beam has a uniform intensity (or radiation fluence) across the field, except in cases using simple beam modifiers, such as wedges or compensators [1].

Advances in computer technology have allowed for the refinement of 3D-CRT into a treatment modality termed *intensity-modulated radiation therapy* (IMRT). IMRT is based on the use of multiple optimized “beamlets” of non-uniform radiation intensity within each single field [2]. Similar to SRS, IMRT requires a high degree of accuracy. By delivering optimized nonuniform intensities within each radiation field, a much higher degree of tumor conformality and normal tissue sparing can be achieved, however. Additionally, in contrast to previous methods of radiotherapy, the use of nonuniform customized fluence distributions with IMRT has the capability of generating concave and other complex dose distributions [2].

Another distinguishing feature of IMRT is the optimization process that takes place during the planning phase. IMRT plans are generated using 3D reverse planning systems by a process known as “inverse planning” or “automated optimization” [2]. First, the physician specifies the goals of treatment, including target volumes, avoidance volumes, and dosimetric parameters (ie, what percentage of the specified volumes should or should not receive what percentage of the prescribed radiation dose). The system then determines the physically deliverable modulated beam fluence profile that results in a dose distribution

* Corresponding author.

E-mail address: marie.davis@hsu.utah.edu
(M.D. Klish).

most closely resembling the one requested by the physician. The idealized treatment differs slightly from the actual computer-generated IMRT plan because of leaf sequencing and machine head radiation leakage [2].

Computer optimization for intensity-modulated radiotherapy

The first step in computer-optimized inverse planning for IMRT is to express the clinical objectives mathematically as an objective function (also called score function or cost function). The objective function can be based on dose and volume constraints or on radiobiologic parameters. Dose-based and dose volume–based objective functions are typically created by minimizing the variance of the deliverable dose relative to the clinically defined dose constraints. This is accomplished by summing the dose contribution from a given number of beamlets that traverse the target and normal tissues. The variance terms for each anatomic structure are summed and multiplied by their importance (or penalty) factors to yield the variance dose- and dose volume–based objective functions. The value of the resulting objective function, often referred to as the score, describes the goodness-of-fit for a plan compared with the defined clinical dose constraints [2].

A weakness of the dose variance model is that it may not adequately account for the radiobiologic response of tissues. For example, if a small number of voxels in a tumor receive an extremely low dose, it may not have a significant effect on the plan's score, although it could have a significant adverse clinical effect, such as treatment failure. Conversely, a small volume of a critical structure that receives an excess radiation dose through a few beamlets may give an acceptable objective dose function but result in significant toxicity. This limitation stems from the fact that the importance factor (representing the penalty imposed for the failure to achieve the prescribed dose) is proportional to the square of the dose variance rather than to the clinical outcome [3].

The limitations of using dose-volume criteria have prompted efforts to develop models for biologic and dose-response criteria that can be used in addition to dose and dose-volume criteria [4–9]. The biologic model optimization is based on the radiobiologic effects produced by a given dose distribution. The objective function is defined by the maximization of tumor control probability (TCP) and minimization of normal tissue compli-

cation probability (NTCP). Unfortunately, the dose response functions of TCP and NTCP in most clinical situations have not been mathematically described with respect to a given dose distribution. Although significant research is currently underway to incorporate radiobiologic objective functions into inverse planning optimization algorithms, such technology is not yet commercially available.

The computerized optimization of a given objective function requires complex mathematical algorithms to describe the interaction of hundreds to thousands of individual beamlets. These algorithms are broadly classified as either iterative or random based on their computational “philosophy.” Iterative algorithms include filtered back projection, linear programming, maximal likelihood, and gradient methods. Simulated annealing and genetic algorithms comprise the random category.

The initial step in iterative algorithms is to track each beamlet from the radiation source through the patient while all other beamlets are set to a weight of 0. The dose in each volume element, or voxel, is calculated for an initial set of beamlet weights. The resulting dose distribution determines the score, or value of the objective function. If the change in beamlet weight results in an improved score, the change is accepted. This process is repeated for all beamlets, presumably resulting in a slight improvement in the plan and at the end of each iteration cycle. Each new beamlet intensity map is used as the basis for subsequent iterations until no further improvement is possible, at which point, the optimal plan is assumed to have been achieved [3].

Random, or stochastic, techniques use non-iterative solutions to optimize a given objective function. Simulated annealing algorithms search out local minima (beamlet configurations that fit the objective function for that beam) within each beam and combine them with all other combinations of local minima for each other beam. A global minima solution is then defined by the optimal combination of local minima [10–13]. There is no guarantee that the absolute optimum will be found, only that the best solution among those examined will be discovered [14–16]. In theory, the advantage of such a complex method is that it may be more likely to find the best solution. In clinical practice, however, the iterative algorithms currently produce plans that are essentially equal to random algorithms in terms of dose-volume histograms (DVHs) for targets and

organs at risk. Moreover, the iterative, or gradient, techniques are by far the most efficient computationally [17–20].

Intensity-modulated radiotherapy delivery

Methods of IMRT delivery include using (1) multileaf collimation (MLC), (2) tomotherapy (slice therapy), and (3) robotic linear accelerators (LINACs) as described below [21].

Multileaf collimation

Computer-controlled allow for precise shaping of radiation fields with individual leaves that range in size from 2 to 15 mm. MLCs with leaf thicknesses less than 5 mm are termed *micro-multileaf collimators* (mMLCs). mMLC devices are thought to provide higher degrees of target conformality and normal tissue sparing for smaller and more complex-shaped targets [2]. IMRT fluence profiles can be created with MLCs using one of three techniques. In the sliding window or dynamic MLC method, opposing MLC leaves sweep across the target volume while the radiation beam is on to create the prescribed intensity modulation within a given field. Alternatively, with the step-and-shoot or segmental MLC method, each field is divided into a series of multiple subfields or segments defined by the collimator leaves and delivered from the same gantry angle. The radiation is turned on only when the leaves have stopped at the appropriate subfield position, resulting in delivery of the desired nonuniform intensity from each gantry angle [22,23]. Another MLC method, intensity-modulated arc therapy, uses multiple fields shaped with the MLC during gantry rotation. The radiation is turned on at intervals of 5° to 10° throughout each arc. The cumulative dose from many superimposed arcs results in the desired intensity-modulated dose distribution [24,25].

Tomotherapy

The commercially available Peacock system (Peacock MIMiC; Nomos Corp, Cranberry Township, PA) is a serial tomotherapy IMRT system in which radiation is delivered with a narrow slit beam measuring approximately 2 cm × 20 cm. The system consists of a temporally modulated binary MLC mounted on a conventional LINAC. Treatment is delivered in contiguous arc strips to adjacent axial slices of the patient. This

requires a high degree of precision in couch motion to avoid overlap of treated arcs or gaps between treated arcs. Low and Mutic [26] reported up to 20% dose error in abutment regions for positioning errors as small as 1mm with such sequential arc IMRT. Carol et al [27] found similar field-matching problems in their analysis of serial tomographic IMRT.

Another form of tomographic IMRT, helical tomography, was proposed and developed by Mackie et al [28] to circumvent the abutment problems inherent in serial tomography [29,30]. Their TomoTherapy HI ART system (Tomotherapy, Madison, WI) differs from serial tomography in that the temporally modulated binary mMLC and LINAC are mounted to a modified CT scanner gantry. The patient is moved through this ring type gantry as IMRT is delivered. There are no abutting treatment arc fields because of the continuous synchronized gantry and table motion. Advantages of this system include its efficiency and the real-time position verification provided by the CT scans obtained during treatment. Because it is a megavoltage machine, however, patients may be exposed to radiation doses on the order of 1 to 3 cGy with each scan.

Robotic linear accelerator

Robotic LINAC systems were first developed for SRS but have now been used for IMRT as well. Webb and his colleagues [31–33] have described conformal IMRT delivered by a robotic LINAC that can move freely in 3D space. This increases the number of possible beam orientations relative to the target compared with other methods of IMRT delivery. For a detailed discussion on robotic LINACs, such as the CyberKnife Stereotactic Radiosurgery System (Accuray, Sunnyvale, CA), readers are referred to the article by Gerszten and Welch in this issue.

Treatment accuracy

Given the steep dose gradients achieved with IMRT, precise dose targeting is paramount. The delivered IMRT dose is determined by multiple factors, including the beamlet weights, beam orientations, couch indices, collimator angles, gantry angle, and patient positioning. Any change in these parameters could lead to a partial target miss or could cause unintended irradiation of sensitive avoidance structures, such as the spinal cord.

Fortunately, among the extracranial organs, the vertebrae and spinal cord have the least breathing-related organ movement as demonstrated by Medin et al [34]. These researchers used stereotactic radiographs of implanted markers in swine and phantom models during inhalation and exhalation to measure vertebral movement. Implanted markers were also observed under continuous fluoroscopy during full respiratory cycles to assess movement. In this analysis, respiration had no detectable influence on vertebral position.

Conversely, patient movement can be a significant contributor to setup error. This point is emphasized by Xing et al [35], who studied the dosimetric effect of small patient movements and treatment machine misalignment in the delivery of IMRT in a nasopharyngeal case and a lumbar spinal case. They found that changes in couch indices or patient positioning errors had a more dramatic effect on the dose distribution than did beam angular misalignment. For example, in their study, a 3-mm movement of the patient in the anterior-posterior direction caused up to a 38% decrease in the minimum target dose and up to a 41% increase in the maximum cord dose, although a 5° change in beam angle caused only a 1.5% decrease in the target minimum or a 5.1% increase in the spinal cord dose. Because the required setup accuracy for paraspinal treatments is often less than 2 mm, minor setup errors can result in the delivery of dangerously high radiation doses to the spinal cord.

Immobilization

Efforts to achieve the required rigid paraspinal target immobilization began with invasive spinal fixation for SRS. Hamilton et al [36–38] devised a stereotactic body frame that attaches to vertebral spinal processes with the patient in the prone position and uses a stereotactic fiducial system for accurate localization. This system was associated with positioning errors on the order of 2 mm (in transverse plane) and less than 4 mm in the longitudinal plane. Although relatively accurate, such invasive measures risk potential surgical complications and can result in a long procedure.

Noninvasive methods of immobilization for extracranial sites, including body vacuum bags, which stabilized patients inside a stereotactic body frame, were not as successful initially [39–41]. Maximal repositioning errors of 7 mm in the transverse plane and 10 mm in the longitudinal

plane, which are unacceptable for paraspinal lesions, have been noted with such systems. The use of a full-body mask attached to a stereotactic body frame allowed up to 3.9 mm of lateral repositioning error in the thoracic spinal area and required hours of preparation time [42].

More recently, technologically advanced and noninvasive means of immobilization have met with success. Researchers at Stanford University demonstrated the technical feasibility of noninvasive radiosurgery for unresectable spinal lesions, including vascular malformations and primary and metastatic spinal tumors using the CyberKnife treatment planning system in 16 patients [43]. The CyberKnife is a frameless image-guided radiosurgery system that relies on reference coordinates in the patient's anatomy or implanted fiducials and not from an external frame. With this system, the target position is measured via orthogonal x-rays at approximately 1- to 2-minute intervals throughout treatment and the beam is automatically realigned to compensate for any target movement. In this study, treatment dose alignment within 1 mm of the target volume was achieved in phantom models. At 6 months of follow-up, there were no complications as a result of the radiosurgery and no clinical or radiographic progression of spinal disease was noted.

Stanford University researchers have also reported on the use of their CyberKnife system for the treatment of 250 cranial, 23 spinal, 9 lung, and 3 pancreatic tumors [44]. In this analysis, treatment sites along the spine were located with reference to the nearest vertebral body using implanted stainless steel fiducials for thoracic and lumbar lesions. A plastic cradle molded to the shape of the patient's back was used to help with immobilization. For cervical spinal lesions, a noninvasive plastic face mask was used for positioning. Controlling the beam direction rather than the patient's position compensated for any residual movement.

Target position records were analyzed revealing that target movement was irregular in amplitude and erratic in occurrence for all sites. The target position along each axis of translation varied by an average of 0.53 mm in the nine spinal cases. The average position fluctuation along all three axes combined was 0.85 mm, which meets the generally accepted targeting standard for spinal radiosurgery. As the authors point out, however, the accumulation of progressive additive targeting errors can only be avoided by regular monitoring and correction of target movement during treatment [44].

Target positioning has also been studied by researchers at the Henry Ford Hospital. They have reported on the accuracy and precision of image-guided single-fraction IMRT for 10 patients with spinal metastases using a noninvasive immobilization device [45]. After receiving conventional radiation to 25 Gy in 10 fractions, a 6- to 8-Gy IMRT single-fraction boost was given to all patients. For the boost planning, infrared-sensitive markers were placed on the patient's skin and vacuum bags or other devices were used as needed to help with patient positioning. Axial CT images were obtained through the target and sent to a dedicated treatment planning system, where the target tumor volume and critical organs, such as the spinal cord, were drawn.

Patients were repositioned for treatment using an automated patient-positioning device consisting of two infrared cameras that detect the infrared sensitive markers on the patient's skin. A computerized control system then compared the marker location with reference information and moved the treatment couch as needed to achieve the preplanned position. Orthogonal x-rays verified patient positioning and were fused with the simulation CT to determine the accuracy of the isocenter.

This sophisticated frameless positioning technology resulted in an isocenter accuracy of 1.36 ± 0.11 mm in the 10 spinal patients studied. The average maximum dose to the anterior edge of the spinal cord was 50% of the prescribed dose. Although not primary end points of this study, the authors noted that all patients had rapid pain relief and improvement in neurologic function [45].

Similarly impressive results have been obtained at Memorial Sloan-Kettering Cancer Center. Yenice et al [46] recently reported the accuracy of paraspinal IMRT using a complex noninvasive immobilization system. A stereotactic body frame, which applies pressure to skeletal points like the pelvic bones, ribs and sternum, was used to immobilize seven patients with thoracic and lumbar spine tumors. Patients were then transferred smoothly on a "railroad-like track system" to a CT scanner, where setup was verified and corrected just before treatment delivery. Based on these pretreatment CT scans, researchers found an average systematic error of 2.0 mm and an average random error of 1.5 mm.

Researchers then retrospectively calculated the impact that these setup errors would have had on patient treatment had they not been corrected with daily CT guidance. The authors report that

such errors, although seemingly small, could have resulted in a greater than 100% prescribed dose to the spinal cord. Using CT guidance, the discrepancy between planned and delivered spinal cord dose was reduced to 10% to 15% [46].

Planning

Many researchers have demonstrated the superiority of IMRT plans over conventional and even 3D-CRT plans. The expectation, which remains to be verified, is that better treatment planning correlates with better patient outcomes.

Verhey [47] performed treatment planning comparisons of conformal and IMRT techniques on paraspinal, prostate, and nasopharyngeal tumors. For all sites, the IMRT plans yielded significantly better dose distributions at the price of additional time and cost. Similarly, researchers from Heidelberg found that IMRT techniques enabled better treatment of paraspinal tumors that wrapped around the spinal cord. They compared a multiple arc segment technique using 3D-CRT consisting of 13 isocentric coplanar beam's eye view-shaped fields with an inverse-planned IMRT technique using seven coplanar equispaced beams. The IMRT plans reduced exposure of normal tissues and improved target coverage compared with the 3D-CRT plans [48].

Researchers from the United Kingdom have compared conventional, 3D-CRT, and IMRT plans to assess target coverage and spinal cord sparing for thyroid carcinomas. IMRT planning achieved the goal dose to the target volume ($P < 0.01$) and reduced the maximum spinal cord dose significantly ($P < 0.01$) compared with conventional and 3D-CRT plans. Authors concluded that IMRT should reduce the risk of myelopathy and may allow dose escalation for patients with thyroid cancer [49]. Later work by De Neve et al [50] showed that dose escalation to thyroid tumors was indeed feasible with IMRT. In this study, patients tolerated doses of up to 80 Gy to primary head and neck or thyroid tumors without exceeding spinal cord tolerance using IMRT.

IMRT plans have consistently demonstrated better dose distributions than conventional and 3D-CRT plans. Although increasing the radiation dose poses a significant technical challenge for target volumes lying close to the spinal cord, clinicians are hopeful that the increased conformality and greater normal tissue sparing resulting from IMRT will enable safe dose escalation for spinal tumors.

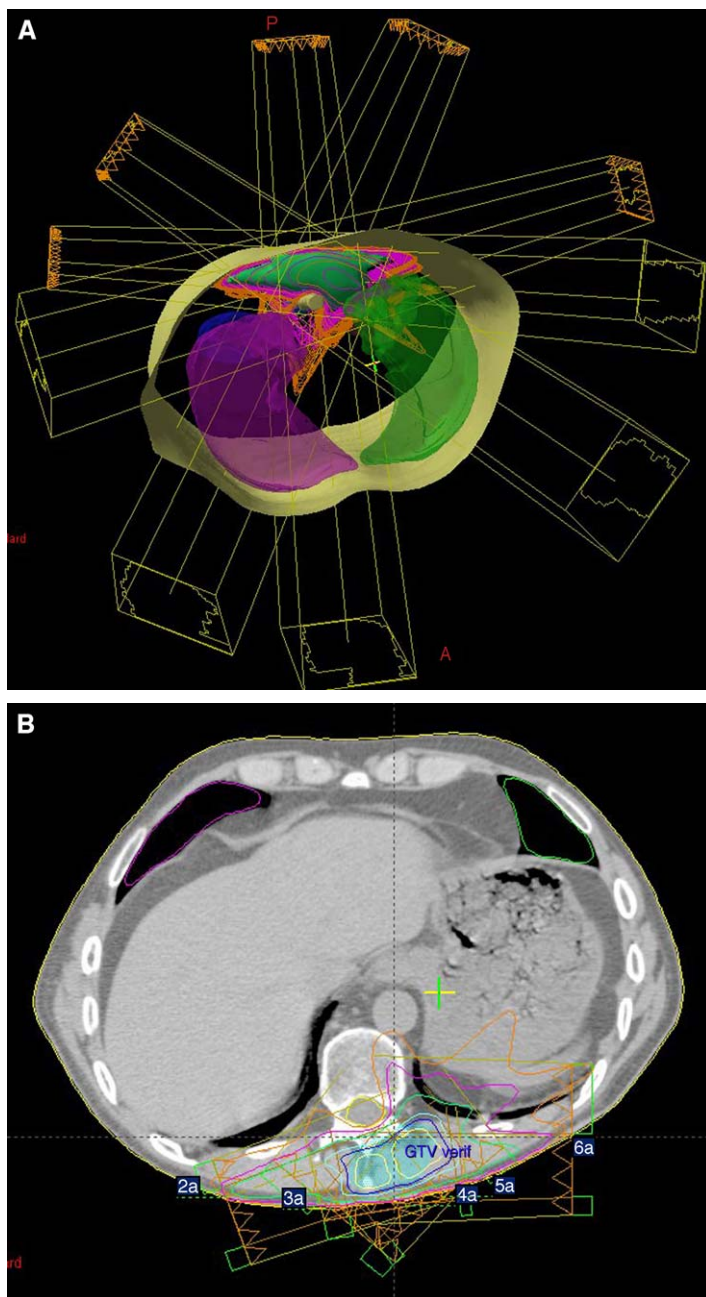


Fig. 1. This is the treatment plan for a 50-year-old man with metastatic lung adenocarcinoma. He developed a painful paraspinous mass at T9 to T10 and had conventional palliative radiotherapy to 3000 cGy in 10 fractions to a field encompassing T9 through T11. His symptoms initially resolved but recurred 8 months later, and he was found to have disease in the T11 and T12 vertebral bodies. Intensity-modulated radiotherapy (IMRT) was used to retreat this area for palliation. (A) Five beams were used with a beam arrangement. Axial (B), sagittal (C), and coronal (D) slices show the isodose lines, highlighting the sharp dose gradient achieved with IMRT. The 97% isodose line covers the entire tumor, whereas the spinal cord receives only 10% of the prescribed dose in all dimensions. This patient was treated with 3750 cGy in 15 daily fractions delivered 5 days per week. He tolerated therapy without complications and experienced pain relief. At 7 months of follow-up, he has no evidence of myelopathy or symptoms of local recurrence and is off all narcotics.

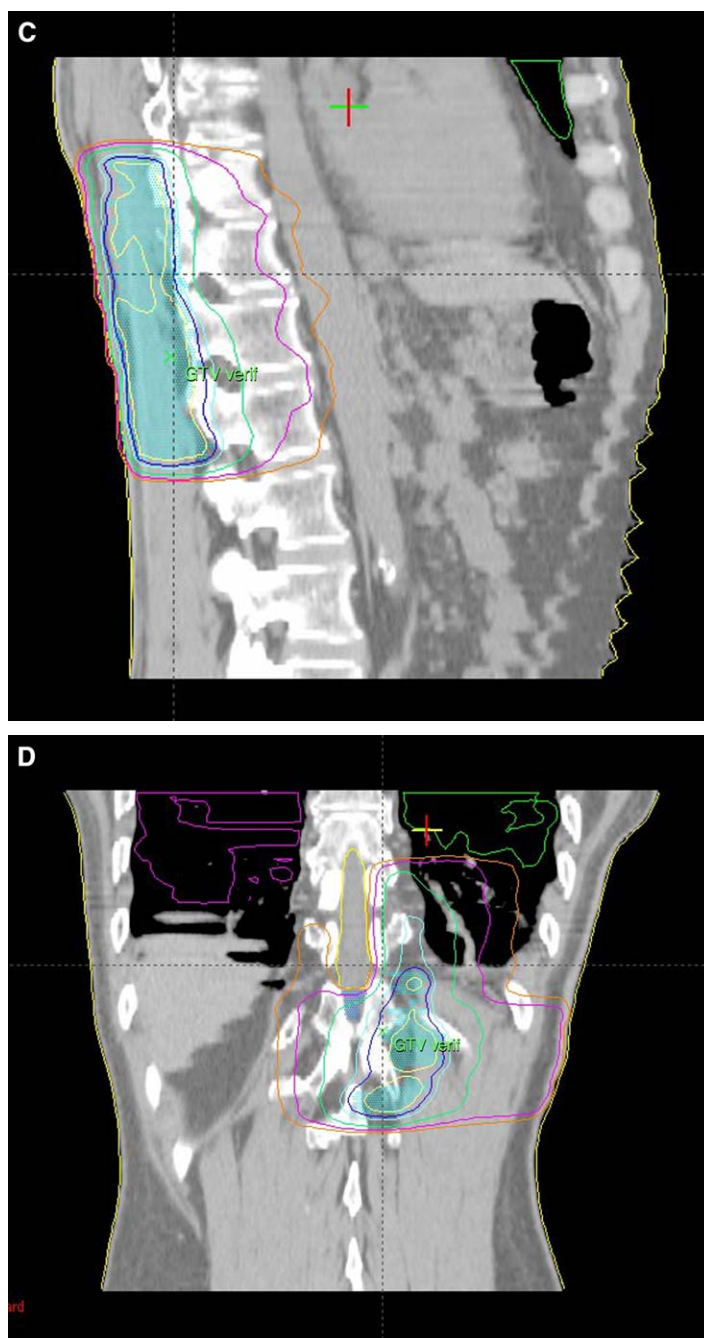


Fig. 1 (continued)

Clinical indications and outcomes

The clinical use of IMRT for paraspinal tumors is a recent development for which long-term clinical follow-up is not available. Notable improvements in local control rates and decreased toxicity have been demonstrated with the use of IMRT for head and neck cancer (HNC), however. For example, researchers at Stanford University report encouraging results from their series of 60 patients with HNC treated with IMRT. At a median follow-up of 17.5 months, 1-year freedom from local regional recurrence rates were 84% for definitive IMRT, 90% for postoperative IMRT, and 82% overall. The 1-year overall survival rates were 83% for definitive IMRT, 100% for postoperative IMRT, and 90% overall [51]. These results compare favorably with historic controls. Similar outcomes have been noted in the University of San Francisco experience with 65 patients treated with definitive radiation for oropharyngeal carcinoma. In this cohort, the 2-year disease-free and overall survival rates were 91% and 89%, respectively [52].

Not only has IMRT improved local control in HNC, but the technique has also reduced morbidity. Fifteen patients treated at the University of Michigan for tumors of the head and neck region derived a significant benefit from contralateral parotid gland sparing from IMRT. Patients were treated with the step-and-shoot IMRT technique, resulting in a 32% dose to the contralateral parotid gland compared with 93% for conventional plans. This resulted in a reduction of xerostomia as measured by unstimulated and stimulated salivary flow before and after radiation and at 3, 6, and 12 months of follow-up [53,54].

Such encouraging results give clinicians hope that IMRT will be a helpful technique for giving useful doses of radiation to the spine. There are small studies with short follow-up that support this notion. Researchers at the University of California, Irvine reported on eight patients who received a total of 10 courses of IMRT to the spine for primary and metastatic lesions. Six courses of IMRT were given as reirradiation, and 4 courses were given for primary management of spinal disease. The mean dose previously received by the spinal cord was 41.5 Gy, with a mean interval from the previous irradiation of 24.7 months. For the reirradiation cases, researchers were able to deliver an additional 28.1-Gy mean dose while limiting the spinal cord to a 58.6-Gy cumulative dose, resulting in a 14% estimated

local control rate at a mean follow-up of 4 months. In the primary irradiation cases, researchers were able to deliver a 59.7-Gy mean dose while limiting the spinal cord maximum dose to a 45.5-Gy mean dose. Of the patients treated with primary intent, the local control rate was 75% at a mean follow-up interval of 9 months. No spinal cord complications were encountered in this series [55].

Likewise, German researchers have shown that IMRT is a safe and effective therapy for previously irradiated, recurrent, or progressive spinal metastases. They report the clinical results of reirradiation of thoracic and lumbar vertebral bone metastases by 3D fractional conformal radiation (FCRT [$n = 5$]) and IMRT ($n = 14$). Patients had previously received radiation to a median dose of 38 Gy. They were reirradiated for tumor progression with pain ($n = 16$) or neurologic symptoms ($n = 12$). The median total dose for reirradiation was 39.6 Gy, but the spinal cord reirradiation dose was less than 20 Gy in all patients. At a median follow-up of 12.3 months from reirradiation, the authors report impressive 6- and 12.3-month overall local control rates of 100% and 94.7%, respectively. At 12.3 months, only 1 patient (who had been treated with FCRT) had failed treatment. The survival rate was 94.2% at 3 months, 82.4% at 6 months, and 64.7% at 12 months, and in most cases, patients died from progressive systemic disease. Significant pain relief was obtained in 13 of 16 patients, and neurologic improvement was achieved in 5 of 12 patients. No clinically significant late toxicity was observed in this study [56]. Fig. 1 illustrates the efficacy of IMRT in sparing the spinal cord during reirradiation for a metastatic vertebral lesion.

Summary

Although promising, many questions remain regarding spinal IMRT. The challenge of patient immobilization must be surmounted before a radiation facility can safely offer spinal IMRT. At many institutions, the increased expense and time requirements from physicists, therapists, and physicians preclude the routine use of IMRT for spinal lesions. Finally, there are no randomized data comparing the safety or efficacy of IMRT with more conventional means of spinal radiation.

Nonetheless, IMRT is one of the most important recent technologic advancements in radiation therapy. For complex treatment problems, such as

spinal tumors, in which the surrounding organs at risk traditionally place significant constraints on the prescription dose, IMRT has great potential to provide the ideal solution.

References

- [1] Yu C, Shepard D. Treatment planning for stereotactic radiosurgery with photon beams. *Technol Cancer Res Treat* 2003;2:93–104.
- [2] Bortfeld TR. Physical optimization. In: Palta JR, Mackie TR, editors. *Intensity-modulated radiation therapy: the state of the art*. Madison, WI: Medical Physics Publishing; 2003. p. 51–77.
- [3] Censor Y. Mathematical optimization for the inverse problem of intensity-modulated radiation therapy. In: Palta JR, Mackie TR, editors. *Intensity-modulated radiation therapy: the state of the art*. Madison, WI: Medical Physics Publishing; 2003. p. 26–50.
- [4] Jackson A, Kutcher GJ. Probability of radiation-induced complications for normal tissues with parallel architecture subject to non-uniform irradiation. *Med Phys* 1993;20:613–25.
- [5] Kallman P, Lind B, Brahme A. An algorithm for maximizing the probability of complication-free tumor control in radiation therapy. *Phys Med Biol* 1992;37:871–90.
- [6] Niemierko A, Goitein M. Calculation of normal tissue complication probability and dose-volume histogram reduction schemes for tissues with a critical element architecture. *Radiother Oncol* 1991;20:166–76.
- [7] Niemierko A, Urie M, Goitein M. Optimization of 3D radiation therapy with both physical and biological end points and constraints. *Int J Radiat Oncol Biol Phys* 1992;23:99–108.
- [8] Niemierko A, Goitein M. Modeling of normal tissue response to radiation: the critical volume model. *Int J Radiat Oncol Biol Phys* 1992;25:135–45.
- [9] Niemierko A, Goitein M. Implementation of a model for estimating tumor control probability for an inhomogeneously irradiated tumor. *Radiother Oncol* 1993;29:140–7.
- [10] Webb S. Optimization of conformal radiotherapy dose distributions by simulated annealing. II. Inclusion of scatter in the 2D technique. *Phys Med Biol* 1991;36:1227–37.
- [11] Webb S. Optimization of conformal radiotherapy dose distributions by simulated annealing of three-dimensional conformal treatment planning for radiation fields defined by a multileaf collimator. *Phys Med Biol* 1991;36:1201–26.
- [12] Mohan R, Mageras GS, Baldwin B, et al. Clinically relevant optimization of 3-D conformal treatments. *Med Phys* 1992;19:933–44.
- [13] Morrill SM, Lane RG, Jacobson G, et al. Treatment planning optimization using constrained simulated annealing. *Phys Med Biol* 1991;36:1341–61.
- [14] Mageras GS, Mohan R. Application of fast simulated annealing to optimization of conformal radiation treatments. *Med Phys* 1993;20:639–47.
- [15] Stein J, Mohan R, Wang X-H, et al. Optimum number and orientations of beams for intensity-modulated treatments [abstract]. *Med Phys* 1996;23:1063.
- [16] Deasy JO. Multiple local minima in radiotherapy optimization problems with dose-volume constraints. *Med Phys* 1997;24:1157–61.
- [17] Bortfeld T. Optimized planning using physical objectives and constraints. *Semin Radiat Oncol* 1999;9:20–34.
- [18] Spirou SV, Chui CS. A gradient inverse planning algorithm with dose-volume constraints. *Med Phys* 1998;25:321–33.
- [19] Xing L, Chen GTY. Iterative algorithms for inverse treatment plan optimization. *Phys Med Biol* 1996;41:2107–23.
- [20] Xing L, Li JG, Pugachev A, et al. Estimation theory and model parameter selection for therapeutic treatment plan optimization. *Med Phys* 1999;26:2348–58.
- [21] Low DA. Physics of intensity modulated radiation therapy for head and neck cancer. In: Chao KS, Ozyigit G, editors. *Intensity modulated radiation therapy for head and neck cancer*. Philadelphia: Lippincott Williams & Wilkins; 2003. p. 1–17.
- [22] Frass BA, Kessler ML, McShan DL, et al. Optimization and clinical use of multisegment IMRT for high dose conformal therapy. *Semin Radiat Oncol* 1999;9:60–77.
- [23] De Neve W, de Wagter C, De Jaeger K, et al. Planning and delivering high dose to targets surrounding the spinal cord at the lower neck and upper mediastinal levels. *Radiother Oncol* 1996;40:271–9.
- [24] Yu CX. Intensity modulated arc therapy with dynamic multileaf collimation: an alternative to tomotherapy. *Phys Med Biol* 1995;40:1435–49.
- [25] Yu C, Symons MJ, Du MN, et al. A method for implementing dynamic photon beam intensity modulation using independent jaws and a multileaf collimator. *Phys Med Biol* 1995;40:769–87.
- [26] Low DA, Mucic S. Abutment region dosimetry for sequential arc IMRT delivery. *Phys Med Biol* 1997;42:1465–70.
- [27] Carol M, Grant W III, Bleier AR, et al. The field-matching problem as it applies to the Peacock three-dimensional conformal system for intensity modulation. *Int J Radiat Oncol Biol Phys* 1996;34:183–7.
- [28] Mackie TR, Holmes T, Swerdeoff S, et al. Tomotherapy: a new concept for the delivery of conformal radiotherapy. *Med Phys* 1993;20:1709–19.

- [29] Mackie TR. Tomotherapy. In: Proceedings of the XII International Conference on the Use of Computers in Radiation Therapy. Salt Lake City; 1997.
- [30] Ruchala KJ, Olivera GH, Schloesser EA, et al. Megavoltage CT on a tomotherapy system. *Phys Med Biol* 1999;44:2597–621.
- [31] Webb S. Conformal intensity modulated radiotherapy (IMRT) delivered by robotic LINAC—conformality versus efficiency of dose delivery. *Phys Med Biol* 2000;45:1715–30.
- [32] Nutting C, Dearnaley DP, Webb S. Intensity modulated radiation therapy: a clinical review. *Br J Radiol* 2000;73:459–69.
- [33] Webb S. Conformal intensity-modulated radiotherapy (IMRT) delivered by robotic LINAC—testing IMRT to the limit? *Phys Med Biol* 1999;44:1639–54.
- [34] Medin PM, Solberg TD, De Salles AF, et al. Investigations of a minimally invasive method for treatment of spinal malignancies with LINAC stereotactic radiation therapy: accuracy and animal studies. *Int J Radiat Oncol Biol Phys* 2002;52:1111–22.
- [35] Xing L, Lin ZX, Donaldson SS, et al. Dosimetric effects of patient displacement and collimator and gantry angle misalignment on intensity modulated radiation therapy. *Radiother Oncol* 2000;56:97–108.
- [36] Hamilton AJ, Lulu BA, Fosmire H, et al. Preliminary clinical experience with linear accelerator-based spinal stereotactic radiosurgery. *Neurosurgery* 1995;36:311–9.
- [37] Hamilton AJ, Lulu B, Fosmire J, Gossett L. LINAC-based spinal stereotactic radiosurgery. *Stereotact Funct Neurosurg* 1996;66:1–9.
- [38] Hamilton AJ, Lulu B, Stea B, Cheng CW, Cassady JR. The use of gold foil wrapping for radiation protection of the spinal cord for recurrent tumor therapy. *Int J Radiat Oncol Biol Phys* 1995;32:507–11.
- [39] Lax I, Blomgren H, Naslund I, et al. Stereotactic radiotherapy of malignancies in the abdomen: methodological aspects. *Acta Oncol* 1994;33:667–83.
- [40] Herfarth KK, Debus J, Lohr F, et al. Extracranial stereotactic radiation therapy: set-up accuracy of patients treated for liver metastases. *Int J Radiat Oncol Biol Phys* 2000;46:329–35.
- [41] Wulf J, Hadinger U, Oppitz U, et al. Stereotactic radiation therapy of extracranial targets: CT-simulation and accuracy of treatment in the stereotactic frame. *Radiother Oncol* 2000;57:225–36.
- [42] Lohr F, Debus J, Frank C, et al. Noninvasive patient fixation for extracranial stereotactic radiotherapy. *Int J Radiat Oncol Biol Phys* 1999;45:521–7.
- [43] Ryu SI, Chang SD, Kim DH, et al. Image-guided hypo-fractionated stereotactic radiosurgery to spinal lesions. *Neurosurgery* 2001;49:838–46.
- [44] Murphy MJ, Chang SD, Gibbs IC, et al. Patterns of patient movement during frameless image-guided radiosurgery. *Int J Radiat Oncol Biol Phys* 2003;55:1400–8.
- [45] Ryu S, Yin FF, Rock J, et al. Image-guided and intensity-modulated radiosurgery for patients with spinal metastasis. *Cancer* 2003;97:2013–8.
- [46] Yenice KM, Lovelock DM, Hunt MA, et al. CT image-guided intensity-modulated therapy for paraspinal tumors using stereotactic immobilization. *Int J Radiat Oncol Biol Phys* 2003;55(3):583–93.
- [47] Verhey LJ. Comparison of three-dimensional conformal radiation therapy and intensity-modulated radiation therapy systems. *Semin Radiat Oncol* 1999;51:257–71.
- [48] Pirzkall A, Lohr F, Rhein B, et al. Conformal radiotherapy of challenging paraspinal tumors using a multiple arc segment technique. *Int J Radiat Oncol Biol Phys* 2000;48(4):1197–204.
- [49] Nutting CM, Convery DJ, Cosgrove VP, et al. Improvements in target coverage and reduced spinal cord irradiation using intensity-modulated radiotherapy (IMRT) in patients with carcinoma of the thyroid gland. *Radiother Oncol* 2001;60(2):173–80.
- [50] De Neve W, De Wagter C, De Jaeger K, et al. Planning and delivering high doses to targets surrounding the spinal cord at the lower neck and upper mediastinal levels: static beam segmentation technique executed with a multileaf collimator. *Radiother Oncol* 1996;40:271–9.
- [51] Yau J, Lieskovsky YC, Horst K, Goffinet DR, Xing L, Pawlicki T, et al. An evaluation of patterns of failure and subjective salivary function in patients treated with intensity-modulated radiotherapy for head and neck cancers [abstract]. *Int J Radiat Oncol Biol Phys* 2003;57:S156.
- [52] Huang K, Lee N, Xia P, et al. Intensity-modulated radiotherapy in the treatment of oropharyngeal carcinoma: a single institutional experience [abstract]. *Int J Radiat Oncol Biol Phys* 2003;57:S302.
- [53] Eisbruch A, Ship JA, Martel MK, et al. Parotid gland sparing in patients undergoing bilateral head and neck irradiation: techniques and early results. *Int J Radiat Oncol Biol Phys* 1996;36:469–80.
- [54] Eisbruch A, Marsh LH, Martel MK, et al. Comprehensive irradiation of head and neck cancer using conformal multisegmental fields: assessment of target coverage and non-involved tissue sparing. *Int J Radiat Oncol Biol Phys* 1998;41:559–68.
- [55] Kuo JV, Cabebe E, Al-Ghazi M, Yakoob I, Ramsinghani NS, Sanford R. Intensity-modulated radiation therapy for the spine at the University of California, Irvine. *Med Dosim* 2002;27:137–45.
- [56] Milker-Zabel S, Zabel A, Thilmann C, Schlegel W, Wannenmacher M, Debus J. Clinical results of retreatment of vertebral bone metastases by stereotactic conformal radiotherapy and intensity-modulated radiotherapy. *Int J Radiat Oncol Biol Phys* 2003;55:162–7.